Magnetohydrodynamic compressible laminar boundary-layer adiabatic flow with adverse pressure gradient and continuous or localized mass transfer

M. Xenos, N. Kafoussias, and G. Karahalios

Abstract: The problem of magnetohydrodynamic compressible boundary-layer flow over a flat plate, in the presence of an adverse pressure gradient, is studied numerically. The fluid is assumed to be Newtonian, electrically conducting and the magnetic field is constant and applied transversely to the direction of the flow. The fluid flow is subjected to a constant velocity of suction and (or) injection, continuous or localized, and there is no heat transfer between the plate and the fluid (adiabatic flow). The system of partial differential equations, describing the problem under consideration, is solved numerically by applying a modification of the Keller box technique. Numerical calculations are carried out for different values of the free-stream Mach number and the magnetic parameter for continuous or localized suction and (or) injection imposed at the wall. The results obtained are shown in the figures and their analysis shows that the flow field can be controlled by the application of a magnetic field as well as by continuous or localized suction and (or) injection.

PACS Nos.: 51.00, 52.00

Résumé : On étudie numériquement le problème de la couche limite compressible magnéto-hydrodynamique sur une plaque plane en présence d' un gradient de pression adverse. Le fluide est supposé être Newtonien, conducteur électrique et le champ magnétique est constant et appliqué perpendiculairement à la direction de l'écoulement. L'écoulement du fluide est sujet à une vitesse constante de succion/injection qui peut être continue ou localisée et il n'existe pas de transfert de chaleur entre la plaque et le fluide (écoulement adiabatique). Le système d'équations différentielles partielles qui décrit le problème est résolu numériquement en utilisant une modification de la méthode « box » de Keller. Des calculs numériques ont été effectués pour différentes valeurs du nombre de Mach d'écoulement libre et du paramètre magnétique pour des conditions de succion/injection continues ou localisées imposées à la surface de la plaque. Les résultats obtenus sont reportés sur des figures et leur analyse a montré que le champ d'écoulement pourrait être contrôlé par l'application du champ magnétique aussi bien que par une suction/injection de fluide continue ou localisée.

Received April 4, 2000. Accepted June 29, 2001. Published on the NRC Research Press Web site on October 2, 2001.

M. Xenos and N. Kafoussias.[1] Department of Mathematics, Section of Applied Analysis, University of Patras, 26500 Patras, Greece.
G. Karahalios. Department of Physics, Section of Theoretical Physics, University of Patras, 26500 Patras, Greece. Telephone: (30-61)-997474

[1] Corresponding author Telephone: (30-61)-997396; FAX: (30-61)-997163; e-mail: nikaf@math.upatras.gr

 DOI: 10.1139/cjp-79-10-1247

1. Introduction

In the past three decades, there has been enormous progress in the study of compressible boundary-layer flow, which is of fundamental importance in many devices encountered in mechanical and aerospace engineering. Because of friction effects, compressible boundary-layer flow tends to have an unpredictable behavior with respect to the designer's ideas about flow around bodies of a given shape, and this unpredictability leads to the general problem of flow control [1]. The flow-control problem becomes more difficult when an adverse pressure gradient is acting on the boundary-layer flow. In such a case, the boundary layer increases its thickness considerably, in the downstream direction, and the flow in it becomes reversed. The term "adverse pressure gradient" means that the pressure increases in the direction of the flow (e.g., $\mathrm{d}P/\mathrm{d}x > 0$) and it may be reversed. Owing to the reversal of the flow, there is considerable thickening of the boundary layer, and associated with it, there is a flow of boundary-layer material into the outside region. When a region with an adverse pressure gradient exists along a wall, the retarded fluid particles cannot, in general, penetrate too far into the region of increased pressure owing to their small kinetic energy. Thus, the boundary layer is deflected sideways from the wall, separates from it, and moves into the main stream. A short distance downstream from the point of separation, the boundary layer becomes so thick that the assumptions that are made in the derivation of the boundary-layer equations no longer apply. So, the boundary layer equations are only valid as far as the point of separation. Separation is mostly an undesirable phenomenon because it entails large energy losses and some representative experimental and numerical studies of a boundary layer with pressure gradients have been presented in refs. 2–4.

It is well recognized that the very effective method for the prevention of separation is boundary-layer suction. It is used in the design of aircraft wings and is also applied to reduce drag [5]. A numerical study of a two-dimensional laminar boundary-layer compressible flow with pressure gradient and heat and mass transfer is presented in ref. 6. It was found that the separation of the boundary layer can be controlled by these techniques because application of suction, or cooling the wall, stabilizes the boundary layer and delays separation.

On the other hand, in recent years, the study of flow and heat transfer for an electrically conducting fluid under the influence of an applied magnetic field has received the attention of many researchers. This is due to its wide application in aerodynamics and in many engineering problems such as MHD (magnetohydrodynamic) generators, plasma studies, nuclear reactors, and those dealing with liquid metals.

Historically, Rossow [7] was the first to study the hydrodynamic behavior of the boundary layer on a semi-infinite flat plate in the presence of a uniform magnetic field. Since then a large amount of literature has been developed on this subject. A review of this topic up to the early eighties can be found in ref. 8.

Boundary-layer models in MHD channels is an attractive research field, with publications of descriptions of a similarity method involving application of a geometric transformation for describing the boundary layer in a flow over an insulating wall [9]. The same models are also used for the study of the unsteady flow of an incompressible, electrically conducting fluid over a porous plate [10] and a convex surface [11]. Calculations of velocity and temperature profiles and heat-transfer rates for a MHD radial wall jet is presented in ref. 12. The effects of Joule heating and viscous dissipation in liquid-metal sliding contacts for high-current applications is discussed in ref. 13. Measurements of the increase in heat flux from a supersonic, high-temperature inert-gas flow to the electrodes of a disk MHD generator, with increasing magnetic fields, is described in ref. 14.

The problem of boundary-layer flow, under the action of an applied magnetic field, has been extensively studied in the case of an incompressible fluid [15–26]. However, in the literature, there seems to be much less documentation of adverse-pressure-gradient effects on the separation of the MHD boundary layer in the presence of mass transfer in the case of a compressible fluid. This is one of the most important problems in boundary-layer theory because in many designs as, for example, in the design of

Fig. 1. Flow configuration and co-ordinate system.

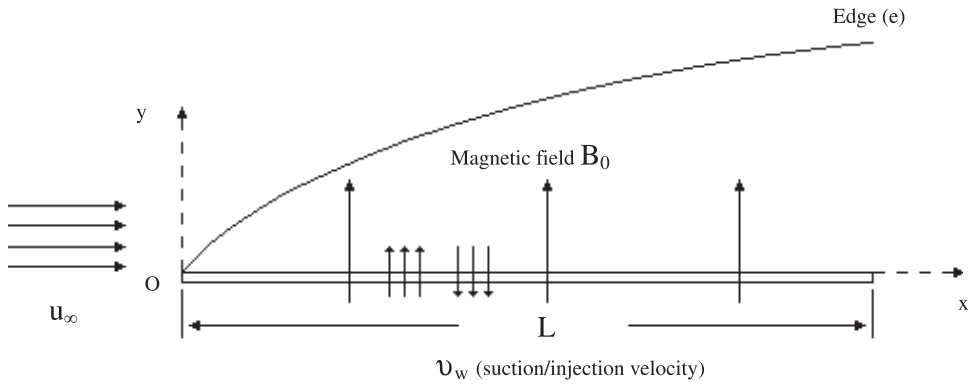

fan blades or airfoils, it is necessary to prevent flow separation to reduce the drag and to produce high lift [1].

The aim of this work is the numerical study of the magnetohydrodynamic, compressible two-dimensional laminar boundary-layer flow, over a permeable flat plate, in the presence of an adverse pressure gradient and mass transfer under adiabatic conditions. The formulation of the problem is presented in Sect. 2, whereas the numerical solution of the problem, for different values of the dimensionless parameters entering the problem under consideration, is given in Sect. 3. Finally, in Sect. 4, an extensive analysis of the results obtained, shown in graphs, is presented.

2. Mathematical formulation of the problem

We consider the steady two-dimensional adiabatic compressible MHD laminar boundary-layer flow over a smooth flat permeable surface. In a Cartesian coordinate system $Oxyz$ the surface is located at

$$y = 0, \qquad 0 \leqslant x \leqslant L, \qquad -\infty < z < +\infty$$

and is parallel to the free-stream of a heat-conducting perfect gas flowing with velocity u_∞ in the positive x-direction (see Fig. 1). The fluid is assumed to be Newtonian and electrically conducting, and the plate is thermally and electrically an insulator or nonconductor. A magnetic field of uniform strength $\boldsymbol{B} = (0, B_0, 0)$ is applied transversely to the direction of the flow. The magnetic field is assumed to be fixed with respect to the plate and the magnetic Reynolds number of the flow is also assumed to be small enough so that the induced magnetic field can be neglected. This is, generally, the case in normal aerodynamic applications. Since no external electric field is applied and the effect of polarization of the ionized fluid is negligible [20], it is also assumed that the electric field $\boldsymbol{E} = \boldsymbol{0}$. Under the above assumptions, the MHD boundary-layer equations, relevant to the problem, are the continuity, momentum, and energy equations, which, in the absence of body forces, can be written as [27,28]

$$\frac{\partial}{\partial x}(\rho u) + \frac{\partial}{\partial y}(\rho \upsilon) = 0 \tag{1}$$

$$\rho u \frac{\partial u}{\partial x} + \rho \upsilon \frac{\partial u}{\partial y} = -\frac{\mathrm{d}p}{\mathrm{d}x} + \frac{\partial}{\partial y}\left(\mu \frac{\partial u}{\partial y}\right) + (\boldsymbol{J}_\mathrm{c} \times \boldsymbol{B})_x \tag{2}$$

$$\rho c_p \left(u \frac{\partial T}{\partial x} + \upsilon \frac{\partial T}{\partial y}\right) = \frac{\partial}{\partial y}\left(k \frac{\partial T}{\partial y}\right) + u \frac{\mathrm{d}p}{\mathrm{d}x} + \mu \left(\frac{\partial u}{\partial y}\right)^2 + \boldsymbol{q} \cdot (\boldsymbol{J}_\mathrm{c} \times \boldsymbol{B}) \tag{3}$$

It is apparent that, according to the boundary-layer theory, the equation of motion normal to the flat plate, the y-momentum equation, has been dropped completely in the above system of equations (1)–(3).

In such a case, the pressure is said to be "impressed" on the boundary layer by the outer potential flow. It may, therefore, be regarded as a known function as far as boundary-layer flow is concerned and it depends only on the coordinate x [27]. On the other hand, the term $\frac{Dp}{Dt}$, in the energy equation (3) for compressible fluids in ref. 27, is represented for the case under consideration by the term $u(\mathrm{d}p/\mathrm{d}x)$.

The boundary conditions of the problem, including a transpiration velocity υ_w at the plate, are

$$y = 0 \ : u = 0, \qquad \upsilon = \upsilon_\mathrm{w}(x), \qquad \frac{\partial T}{\partial y} = 0 \, (\dot{q}_\mathrm{w} = 0) \, , \qquad y \to \delta \ : u = u_\mathrm{e}(x), \qquad T = T_\mathrm{e}(x) \tag{4}$$

In the above equations ρ is the density of the gas; u, υ are the velocity components along the x- and y-axis, respectively ($\boldsymbol{q} = (u, \upsilon)$); p is the pressure; T is the temperature of the gas in the boundary layer; μ is the viscosity; k is the coefficient of thermal conductivity; c_p is the specific heat; δ is the boundary-layer thickness; u_e, T_e are the fluid velocity component and temperature at the edge of the boundary layer, respectively; σ is the electrical conductivity and is assumed to be constant; $\boldsymbol{J}_\mathrm{c}$ is the conduction current; and $\boldsymbol{B}$ is the magnetic field strength. The conduction current in our case is defined as

$$\boldsymbol{J}_\mathrm{c} = \sigma \, (\boldsymbol{q} \times \boldsymbol{B}) \qquad (\boldsymbol{E} = \boldsymbol{0}) \tag{5}$$

where $\boldsymbol{q} = (u, \upsilon)$ is the velocity field. So, the last term in (2) is the Lorentz force, which for the problem under consideration becomes

$$(\boldsymbol{J}_\mathrm{c} \times \boldsymbol{B})_x = -\sigma \, u B_0^2 \tag{6}$$

whereas the last term in (3) is the Joule-heating term, which becomes

$$\frac{\boldsymbol{J}_\mathrm{c} \cdot \boldsymbol{J}_\mathrm{c}}{\sigma} = \sigma \, u^2 B_0^2 \tag{7}$$

In MHD, the current, which depends on the strength of the magnetic field, produces Joule heating in the fluid and is, in general, of the same order as the viscous dissipative heat. The last two terms on the right-hand side of (3) signify, respectively, heat generated by friction (or viscous dissipative heat) and Joule heating [28–30].

Under the above assumptions, the equations of the problem under consideration can now be written as

$$\frac{\partial}{\partial x}(\rho u) + \frac{\partial}{\partial y}(\rho \upsilon) = 0 \tag{8}$$

$$\rho u \frac{\partial u}{\partial x} + \rho \upsilon \frac{\partial u}{\partial y} = -\frac{\mathrm{d}p}{\mathrm{d}x} + \frac{\partial}{\partial y}\left(\mu \frac{\partial u}{\partial y}\right) - \sigma B_0^2 u \tag{9}$$

$$\rho \, c_p \left(u \frac{\partial T}{\partial x} + \upsilon \frac{\partial T}{\partial y}\right) = \frac{\partial}{\partial y}\left(k \frac{\partial T}{\partial y}\right) + u \frac{\mathrm{d}p}{\mathrm{d}x} + \mu \left(\frac{\partial u}{\partial y}\right)^2 + \sigma B_0^2 u^2 \tag{10}$$

whereas the boundary conditions (4) remain the same.

Introducing H as the sum of the thermal and kinetic energy (total energy) per unity mass of the fluid defined, for a perfect gas, by the expression $H = c_p T + \frac{1}{2}u^2$, we add (9) multiplied by u to (10). Then the system of equations for the problem becomes

$$\frac{\partial}{\partial x}(\rho u) + \frac{\partial}{\partial y}(\rho \upsilon) = 0 \tag{11}$$

$$\rho u\frac{\partial u}{\partial x}+\rho \upsilon\frac{\partial u}{\partial y}=-\frac{\mathrm{d}p}{\mathrm{d}x}+\frac{\partial}{\partial y}\left(\mu\frac{\partial u}{\partial y}\right)-\sigma B_0^2 u \tag{12}$$

$$\rho u\frac{\partial H}{\partial x}+\rho \upsilon\frac{\partial H}{\partial y}=\frac{\partial}{\partial y}\left[\frac{\mu}{Pr}\frac{\partial H}{\partial y}+\mu\left(1-\frac{1}{Pr}\right)u\frac{\partial u}{\partial y}\right] \tag{13}$$

where Pr is the Prandtl number defined as $Pr=\mu\, c_p/k$.

The boundary conditions (4) can be written now as

$$y=0\ :u=0,\qquad \upsilon=\upsilon_{\mathrm{w}}(x),\qquad \frac{\partial H}{\partial y}=0,\qquad y\to\delta\ :u=u_{\mathrm{e}}(x),\qquad H=H_{\mathrm{e}}(x) \tag{14}$$

where

$$H_{\mathrm{w}}(x)=c_pT_{\mathrm{w}}(x)\ \text{ and }\ H_{\mathrm{e}}(x)=c_pT_{\mathrm{e}}(x)+\frac{1}{2}u_{\mathrm{e}}^2(x) \tag{15}$$

By using Bernoulli's equation, for the case of magnetohydrodynamic flow [28],

$$-\frac{\mathrm{d}p}{\mathrm{d}x}=\rho_{\mathrm{e}}u_{\mathrm{e}}\frac{\mathrm{d}u_{\mathrm{e}}}{\mathrm{d}x}+\sigma\, B_0^2u_{\mathrm{e}} \tag{16}$$

where the subscript "e "refers to the conditions at the edge of the boundary layer, (12) can be now written as

$$\rho u\frac{\partial u}{\partial x}+\rho \upsilon\frac{\partial u}{\partial y}=\rho_{\mathrm{e}}u_{\mathrm{e}}\frac{\mathrm{d}u_{\mathrm{e}}}{\mathrm{d}x}+\sigma\, B_0^2u_{\mathrm{e}}+\frac{\partial}{\partial y}\left(\mu\frac{\partial u}{\partial y}\right)-\sigma\, B_0^2u \tag{17}$$

The steady two-dimensional compressible MHD laminar boundary-layer flow, of the problem under consideration, is finally described by the following equations:

$$\frac{\partial}{\partial x}(\rho u)+\frac{\partial}{\partial y}(\rho\upsilon)=0 \tag{18}$$

$$\rho u\frac{\partial u}{\partial x}+\rho \upsilon\frac{\partial u}{\partial y}=\rho_{\mathrm{e}}u_{\mathrm{e}}\frac{\mathrm{d}u_{\mathrm{e}}}{\mathrm{d}x}+\frac{\partial}{\partial y}\left(\mu\frac{\partial u}{\partial y}\right)-\sigma\, B_0^2\,(u-u_{\mathrm{e}}) \tag{19}$$

$$\rho u\frac{\partial H}{\partial x}+\rho \upsilon\frac{\partial H}{\partial y}=\frac{\partial}{\partial y}\left[\frac{\mu}{Pr}\frac{\partial H}{\partial y}+\mu\left(1-\frac{1}{Pr}\right)u\frac{\partial u}{\partial y}\right] \tag{20}$$

and the boundary conditions

$$y=0\ :u=0,\qquad \upsilon=\upsilon_{\mathrm{w}}(x),\qquad \frac{\partial H}{\partial y}=0,\qquad y\to\delta\ :u=u_{\mathrm{e}}(x),\qquad H=H_{\mathrm{e}}(x) \tag{21}$$

The system of equations (18)–(21) constitutes a coupled and nonlinear system of partial differential equations with the unknown functions $u=u(x,y)$, $\upsilon=\upsilon(x,y)$, and $H=H(x,y)$ defined in the rectangular domain $D=\{(x,y)/0<x<L, 0<y<\infty\}$. So, to solve the system numerically, it is useful to express it in transformed variables. For this purpose, the compressible version of the Falkner–Skan transformation is introduced, defined by

$$\eta=\int_0^y\left(\frac{u_{\mathrm{e}}(x)}{\nu_{\mathrm{e}}(x)\,x}\right)^{1/2}\frac{\rho(x,y)}{\rho_{\mathrm{e}}(x)}\,\mathrm{d}y\ ,\qquad \psi(x,y)=(\rho_{\mathrm{e}}\mu_{\mathrm{e}}u_{\mathrm{e}}x)^{1/2}f(x,\eta) \tag{22}$$

where $\nu_{\mathrm{e}}(x)$ is the kinematic viscosity at the edge of the boundary layer and *f(x,η)* is the dimensionless stream function.

The Falkner–Skan transformation, defined by the above relations, can be used to reduce the boundary-layer equations to ordinary differential equations for similar flows. It can also be used for nonsimilar flows for convenience in numerical work, because it reduces, if it does not eliminate, dependence on x [31].

Defining the dimensionless total energy ratio S as H/H_e and by using the definition of the stream function ψ, for a compressible flow, that satisfies the continuity equation (18), with the relations

$$\rho u = \frac{\partial \psi}{\partial y}, \qquad \rho \upsilon = -\frac{\partial \psi}{\partial x} \tag{23}$$

the system of equations (19)–(21) becomes

$$(bf'')' + m_1 ff'' + m_2[c - (f')^2] = x\left[m_3\left(f' - 1\right) + f'\frac{\partial f'}{\partial x} - f''\frac{\partial f}{\partial x}\right] \tag{24}$$

$$(e\,S' + d\,f'\,f'')' + m_1 f\,S' = x\left(f'\frac{\partial\, S}{\partial\, x} - S'\frac{\partial\, f}{\partial\, x}\right) \tag{25}$$

$$\begin{aligned} &\eta = 0: \quad f' = 0,\ f_w = f(x,0) = -\frac{1}{(u_e\mu_e\rho_e x)^{1/2}}\int_0^x \rho_w \upsilon_w(x)\,\mathrm{d}x,\ S'_w = 0 \\ &\eta = \eta_e: \quad f' = 1,\ S = 1 \end{aligned} \tag{26}$$

where η_e is the dimensionless thickness of the boundary layer; primes denote partial differentiation with respect to $\eta\left(()' = \frac{\partial()}{\partial\eta}\right)$; and the quantities b, m_1, m_2, m_3 etc. are defined as follows:

$$\begin{aligned} &b = C, \quad C = \frac{\rho\mu}{\rho_e\mu_e}, \quad c = \frac{\rho_e}{\rho}, \quad d = \frac{Cu_e^2}{H_e}\left(1 - \frac{1}{Pr}\right), \quad e = \frac{b}{Pr}, \quad S = \frac{H}{H_e} \\ &m_1 = \frac{1}{2}\left[1 + m_2 + \frac{x}{\rho_e\mu_e}\frac{\mathrm{d}}{\mathrm{d}x}(\rho_e\mu_e)\right],\ m_2 = \frac{x}{u_e}\frac{\mathrm{d}u_e}{\mathrm{d}x},\ R_x = \frac{u_e x}{\nu_e},\ m_3 = \frac{m_0 c}{\rho_e\, u_e},\ m_0 = \sigma\, B_0^2 \end{aligned} \tag{27}$$

So, the problem under consideration is described by the system of equations (24) and (25), subjected to the boundary condition (26), whereas the various coefficients entering into these equations are defined by the expressions (27).

The coefficient m_3 is called the "magnetic parameter" and it is worth mentioning that in the absence of an applied magnetic field ($m_0 = 0$) the first term on the right-hand side of the momentum equation (24) disappears, enabling us to make a comparative study with the aerodynamic case that has already been studied in ref. 6.

3. Numerical solution of the problem

The aim of this work is to investigate the effect of an applied magnetic field on the steady two-dimensional adiabatic compressible MHD laminar boundary-layer flow over a smooth flat permeable surface in the presence of an adverse pressure gradient. To show this effect on the flow field in the presence of an adverse pressure gradient we consider, as in ref. 6, the linearly retarded flow, known as Howarth's flow, in which the external velocity varies linearly with x, that is,

$$u_e(\bar{x}) = u_\infty(1 - \bar{x}) \tag{28}$$

where u_∞ is the free-stream velocity; $\bar{x} = x/L$, and L is the length of the boundary porous plate. This flow model can be interpreted, for instance, as representing the potential flow along a flat wall that starts

at $\bar{x} = 0$ and that abuts on to another infinite wall at right angles to it at $\bar{x} = 1$ ($x = L$) [27]. This is a usual pattern of flow in modern aerospace engineering and aerodynamics devices that improves the aircraft's performance over a wide range of speed [32]. In such a case, the adverse pressure gradient $-\frac{\mathrm{d}p}{\mathrm{d}x}$, defined by (16), is a function of x. For the numerical calculations the length, L is taken equal to 8 m so that x varies between $x = 0$ and 8 m.

The numerical scheme used to solve the system of equations (24)–(27) is a modified version of the Keller-box method described in detail in ref. 6.

Numerical calculations were carried out for air, at about $T_\infty = 300$ K ($Pr = 0.708$), for $S'_\mathrm{w} = 0$, $\big(S'(0) = 0\big)$, thus covering the case in which there is no heat transfer between the plate and the fluid (adiabatic). It is worth mentioning here that the case in which the dimensionless heat-transfer parameter $S'_\mathrm{w} \neq 0$ corresponds to a flow with heat transfer between the plate and the fluid, whereas the requirement $S'_\mathrm{w} = 0$ corresponds to a flow with no heat transfer between the wall and the fluid (adiabatic flow). So, to examine exclusively the influence of the applied magnetic field on the flow field, in the presence of mass transfer, we study only the case where $S'_\mathrm{w} = 0$ (adiabatic).

In recent years, suction has very often been used as an aerodynamic flow control technique to prevent laminar to turbulent boundary-layer transition as well as turbulent flow separation. Application of suction along the leading edge of a wing stabilizes the boundary layer and prevents transition from laminar to turbulent flow over the wing [5]. Small amounts of suction are very efficient for transition control because this technique increases the stabilizing properties of the laminar boundary layer by changing the shape of the mean velocity profiles [33]. However, if the suction velocity υ_w is too large the boundary layer could be very thin and the roughness effects could be enhanced. As a result, negative effects in terms of drag reduction could be recovered [1]. In our case, the suction and (or) injection velocity at the wall, υ_w, was taken as constant and equal to $\upsilon_\mathrm{w} = \mp 10^{-5} u_\infty$, which is a valid assumption to ensure that the flow with suction or injection at the wall satisfies the simplifying conditions that form the basis of the boundary layer theory [27]. Also, υ_w represents the velocity of suction or injection at the wall according as $\upsilon_\mathrm{w} < 0$ or $\upsilon_\mathrm{w} > 0$, respectively. The case $\upsilon_\mathrm{w} = 0$ corresponds to an impermeable wall (no suction and (or) injection).

On the other hand, it is known that a large suction volume is uneconomical because a large proportion of the savings in power, due to the reduction in drag or to the removal of the separation point downstream, is then used to drive the suction pump. It is, therefore, important to determine the minimum suction volume or the location of the suction zone, in the case of localized suction, that is required to control the boundary-layer flow. Interesting information concerning the influence of the suction location on the stability in the boundary layers has been obtained using the nonlinear parabolized stability equations (PSE) approach [5]. The results obtained were related to a flat plate flow with a free stream velocity of 50 m/s. Suction was applied over a streamwise extent of 10 cm with a vertical suction velocity υ_w equal to -1 cm/s. Also, fundamental wind tunnel experiments performed by Reynolds and Saric [5] indicated that suction is more effective when applied at Reynolds numbers close to the lower branch of the neutral curve, in qualitative agreement with previous theoretical results. Finally, measurements carried out on an 8% thick symmetrical aerofoil showed that continuous suction is most effective when it is confined to the upper side of the wing and when it extends over a region of $0.15L$ approximately [27]. So, to examine the influence of localized suction and (or) injection on the laminar boundary layer in our study, we also applied continuous suction and (or) injection in a region confined between $x = \alpha = x_\mathrm{s} - s$ and $x = b = x_\mathrm{s} + s$ where x_s is the stream wise location of the center of the slot and $2s$ is the width of the slot [34]. To avoid difficulties associated with discontinuities in the region of the boundary surface, simple smoothing functions can be introduced for the suction and (or) injection velocity $\upsilon_\mathrm{w}(x)$ at the wall, which can be written as [31]

$$\upsilon_\mathrm{w}(x) = \frac{1}{2}\upsilon_0[1 + \tanh\beta\,(x - a)], \qquad 0 < x \leqslant \frac{a+b}{2} = x_\mathrm{s} \tag{29}$$

and

$$\upsilon_{\mathrm{w}}(x) = \frac{1}{2}\upsilon_0[1 - \tanh\beta\,(x-b)], \qquad x > \frac{a+b}{2} = x_{\mathrm{s}} \tag{30}$$

where $\beta = 10$ and υ_0 is a constant suction and (or) injection velocity depending on whether $\upsilon_0 < 0$ or $\upsilon_0 > 0$, respectively. It is also possible to apply a Gaussian distribution for the suction and (or) injection velocity given by the expression

$$\upsilon_{\mathrm{w}}(x) = \mp A_{\mathrm{s}}\,\mathrm{e}^{-(x-x_{\mathrm{s}})^2/s^2} \tag{31}$$

where A_{s} is the suction and (or) injection strength. In such a case, the fluid volume flux through the slot is $\sqrt{\pi}\,s^2 A_{\mathrm{s}}$. In our study, for the case of localized suction and (or) injection we applied (31) for the velocity $\upsilon_{\mathrm{w}}(x)$ with $A_{\mathrm{s}} = 5 \times 10^{-5} u_\infty$, $s = 0.1$ for different values of x_{s}.

The free-stream values μ_∞, u_∞, ρ_∞, and H_∞ were calculated from the formulas [31]

$$\mu_\infty = \frac{1.45 \times 10^{-6} T_\infty^{3/2}}{(T_\infty + 110.33)} \qquad \text{(Sutherland's law)} \tag{32}$$

$$u_\infty = 20.04 M_\infty \sqrt{T_\infty} \tag{33}$$

$$\rho_\infty = \frac{p_\infty}{287 T_\infty} \tag{34}$$

$$H_\infty = 1005.7 T_\infty + \frac{1}{2}u_\infty^2 \qquad (c_p = 1005.7) \tag{35}$$

for different values of the free-stream Mach number $M_\infty (M_\infty = 0.375, 0.75, 1.5)$, whereas the edge values T_{e} and p_{e} were calculated using the formulas

$$T_{\mathrm{e}} = T_\infty \left\{ 1 - \frac{\gamma - 1}{2} M_\infty^2 \left[\left(\frac{u_{\mathrm{e}}}{u_\infty} \right)^2 - 1 \right] \right\}, \qquad p_{\mathrm{e}} = p_\infty \left(\frac{T_{\mathrm{e}}}{T_\infty} \right)^{\gamma/(\gamma-1)} \tag{36}$$

where $\gamma = c_p/c_v = 1.4$.

The edge values μ_{e}, ρ_{e}, and H_{e} were calculated by using formulas identical to those given by (32), (34), and (35), respectively, except that free stream values (∞) of temperature, pressure, and velocity were replaced by their edge values (e). It is worth mentioning here that Sutherland's law is an adequate approximation for the variation of viscosity μ with temperature T, for air [35].

In MHD boundary-layer problems the "magnetic parameter" m_3, defined as $m_3 = \frac{m_0 c}{\rho_{\mathrm{e}} u_{\mathrm{e}}}$, where $c = \frac{\rho_{\mathrm{e}}}{\rho}$ and $m_0 = \sigma\, B_0^2$, plays an important role and represents the influence of the applied magnetic field on the flow field. Defining the local Hartmann number as $Ha_x = \left(\frac{\sigma\, B_0^2}{\mu_{\mathrm{e}}} \right)^{1/2} x$, it can be shown that the **magnetic parameter** $m^* = m_3 x$ is related to the viscous local Reynolds number R_x and the local Hartmann number Ha_x by the relation

$$m^* = m_3 x = c \frac{Ha_x^2}{R_x} \tag{37}$$

and is, actually, the ratio of the electromagnetic forces to the inertial forces acting on the fluid elements. So, the results of this work, concerning the velocity field, the temperature field, and coefficient of skin friction (wall-shear parameter), are obtained for $Pr = 0.708$ (air), for different values of Mach number M_∞, and for the magnetic parameter m^* (m_0) for the case of localized as well as continuous suction and (or) injection.

Fig. 2. Variations of the dimensionless velocity profiles $f'(\eta)$ for $M_\infty = 0.5$; $\upsilon_w = 0$; $m_0 = 0$, 4, and 8.

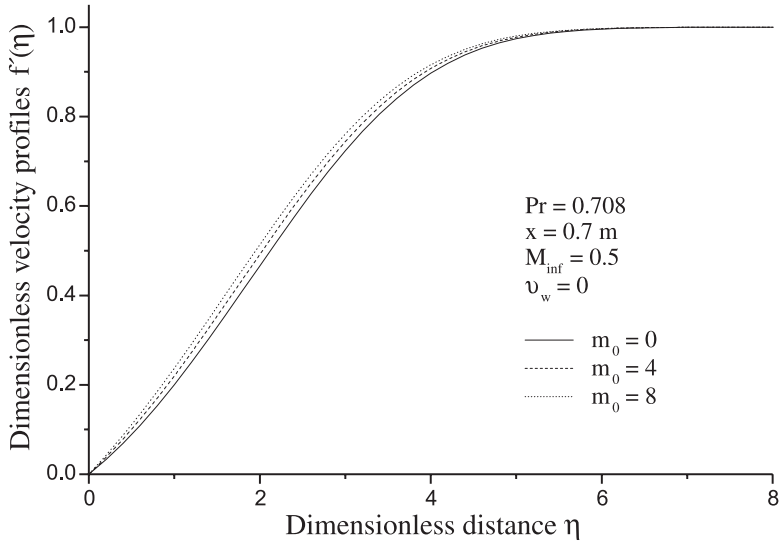

Fig. 3. Variations of the dimensionless velocity profiles $f'(\eta)$ for $M_\infty = 0.5$ and 1.5, $\upsilon_w = 0$, $m_0 = 0$ and 8.

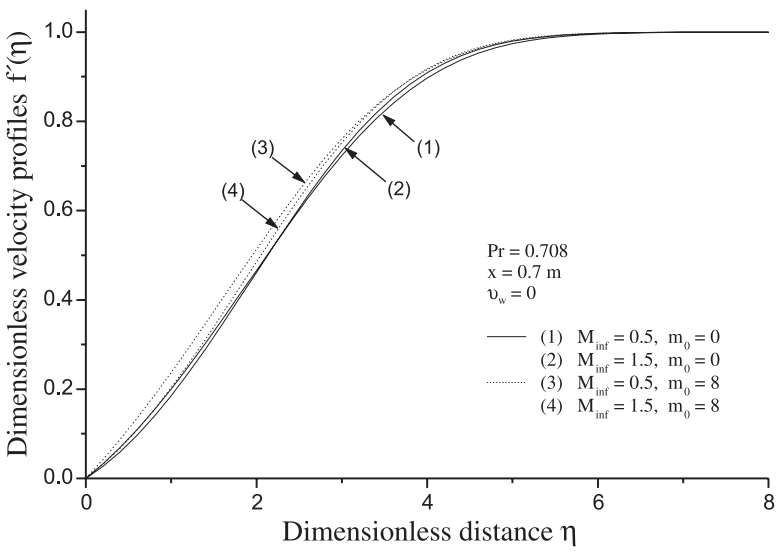

In our case we consider that $\sigma = 1$ mho/m, which is an acceptable value for the electrical conductivity of air, and for the applied magnetic field B_0 we assume values up to 3.0 Wb/m^2, which is also an acceptable value, since the magnetic field is considered fixed with respect to the plate [7]. Under these assumptions, the quantity $m_0 = \sigma B_0^2$ can vary from 0.0 to 9.0 $\left(\frac{\text{mho}}{\text{m}}\frac{\text{Wb}}{\text{m}^2}\right)$ and these values have been given in our problem.

4. Results and discussion

The numerical results obtained, concerning the dimensionless velocity profiles $f'(x, \eta)$, the dimensionless total energy (temperature) profiles $S(x, \eta)$, and especially the dimensionless skin friction

Fig. 4. Variations of the dimensionless velocity profiles $f'(\eta)$ for $M_\infty = 0.5$; $m_0 = 4.0$; and $\upsilon_w = 0$, <0, >0.

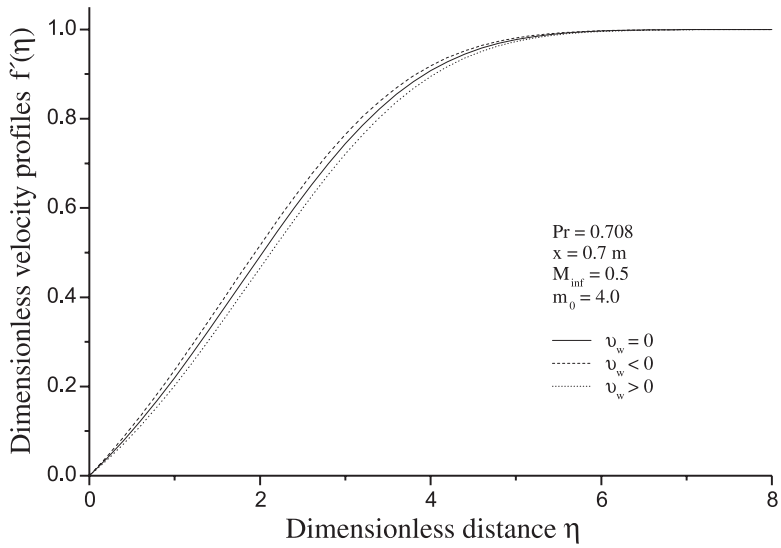

Fig. 5. Variations of the dimensionless velocity profiles $f'(\eta)$ for $M_\infty = 0.5$; $m_0 = 0$ and 8; and $\upsilon_w = 0$, <0, >0.

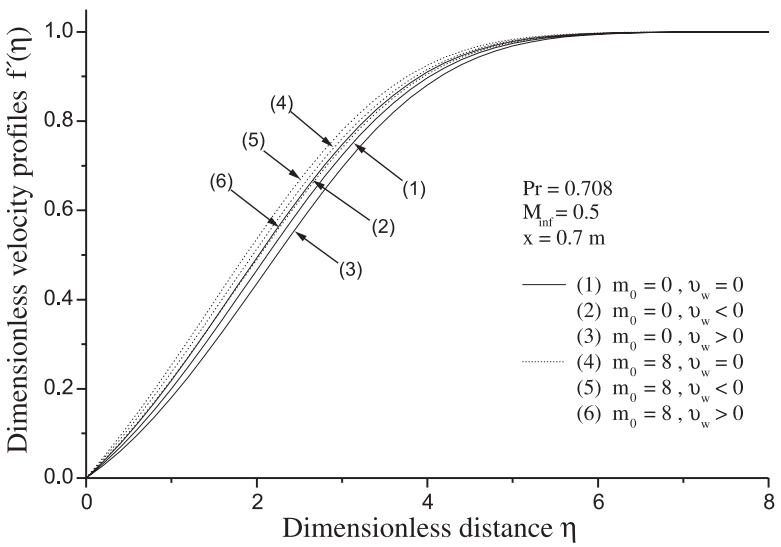

coefficient $f''_w(x) = f''(x, 0)$, are shown in the figures for different values of the dimensionless parameters entering the problem under consideration. These results are presented for the case of suction and (or) injection, continuous or localized, as well as for the case of an impermeable wall ($\upsilon_w = 0$) in the case of air ($Pr = 0.708$) and for different values of the free stream Mach number $M_\infty = M_{\inf}$ and the magnetic parameter m_3 or $m_0 = \sigma B_0^2$. The case $m_0 \neq 0$ corresponds to magnetohydrodynamic flow whereas the case $m_0 = 0$ corresponds to the hydrodynamic one. To examine the influence of the suction and (or) injection and the magnetic field on the flow field, we consider only the case of an adiabatic flow $\left(S'_w = 0\right)$, e.g., of a flow in which there is no heat transfer between the plate and the fluid. However, similar results can be obtained for the case of heating the wall ($S_w > 1$) or for the case of cooling the wall ($S_w < 1$).

Fig. 6. Variations of the dimensionless temperature profiles $S(\eta)$ for $M_\infty = 0.5$; $\upsilon_w = 0$; $m_0 = 0$, 4, and 8.

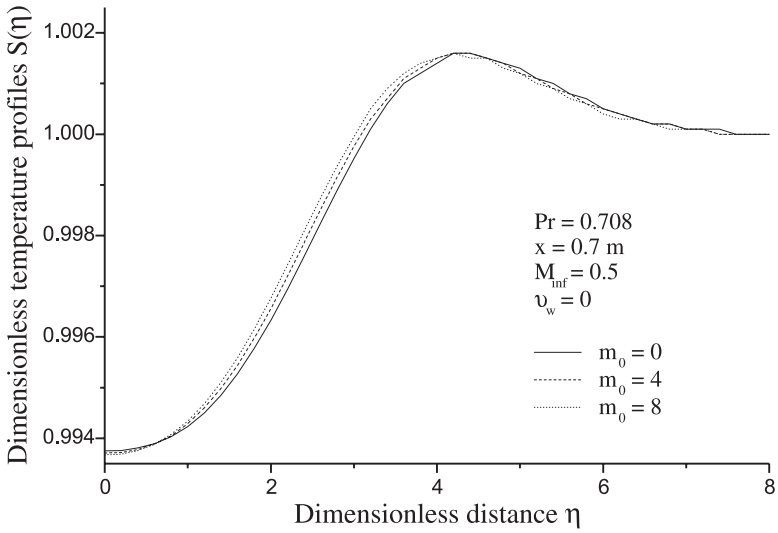

It is worth mentioning here that the dimensionless total energy ratio S is defined by the expression $S = H/H_e$, where H is the total energy of the fluid, e.g., $H = c_p T + \frac{1}{2}u^2$. It is apparent then that the case $S_w = \frac{H_w}{H_e} > 1$ (heating of the wall) actually means that $c_p\,(T_w - T_e) > \frac{1}{2}u_e^2$, whereas the case $S_w < 1$ (cooling of the wall) means that $c_p\,(T_w - T_e) < \frac{1}{2}u_e^2$. The case $S_w = 1$, or more precisely, $S'_w = 0$ corresponds to an adiabatic flow.

The variations of the dimensionless velocity profiles $f'(x, \eta)$, at a typical distance $x = 0.7$ m from the leading edge of the wall, are shown in Figs. 2–5. Figure 2 shows the variations of $f'(\eta)$ for $M_\infty = 0.5$ for the case of an impermeable wall ($\upsilon_w = 0$) and for different values of the magnetic parameter m_0. It is observed that application of the magnetic field accelerates the air motion inside the boundary layer. This influence of the magnetic field on the velocity field decreases as the free-stream Mach number increases (Fig. 3). Quantitatively, when $\eta = 3$ and $M_\infty = 0.5$ application of the magnetic field helps in increasing $f'(\eta)$ by 5.17% , whereas the corresponding increase in the case $M_\infty = 1.5$ is only 3.92% . Also, application of suction ($\upsilon_w < 0$) increases the velocity of the fluid inside the boundary layer and modifies the shape of the velocity profile (Fig. 4). This modification is such that, as we shall see later in the case of skin friction coefficient (Figs. 10–14), the separation point x^* moves down the plate. However, the opposite is true in the case of injection ($\upsilon_w > 0$). The combined influence of the magnetic field and of the suction and (or) injection technique for the control of the boundary layer is shown in Fig. 5. It is worth mentioning here that when $\eta = 3$, $m_0 = 0$, and $\upsilon_w > 0$ (curve (3)) there is a 10.68% reduction in the fluid velocity with respect to the corresponding one (curve (5)) for the case of suction ($\upsilon_w < 0$) in the presence a of magnetic field ($m_0 = 8$).

The variations of the total energy ratio or the dimensionless "temperature" $S = H/H_e$, for a typical distance $x = 0.7$ m from the leading edge of the plate, are plotted against the dimensionless distance η through the boundary layer in Figs. 6–9 for different values of the magnetic parameter m_0, the free-stream Mach number M_∞, for the case of suction and (or) injection, and of an impermeable plate ($\upsilon_w = 0$). Since the flow is assumed to be adiabatic and there is no heat transfer between the plate and the fluid $\left(S'_w = 0\right)$ the temperature increase inside the thermal boundary layer is exclusively due to friction and Joule heating. It is observed in all these figures that initially the fluid temperature rises and attains the maximum value in the thermal boundary layer and then decreases approaching asymptotically to its limiting value at infinity. This variation of the fluid temperature is more evident for higher values of the free-stream Mach number (Fig. 7). It is apparent that in the neighbourhood of the wall and in the

Fig. 7. Variations of the dimensionless temperature profiles $S(\eta)$ for $M_\infty = 0.5$ and 1.5, $\upsilon_w = 0$, $m_0 = 0$ and 8.

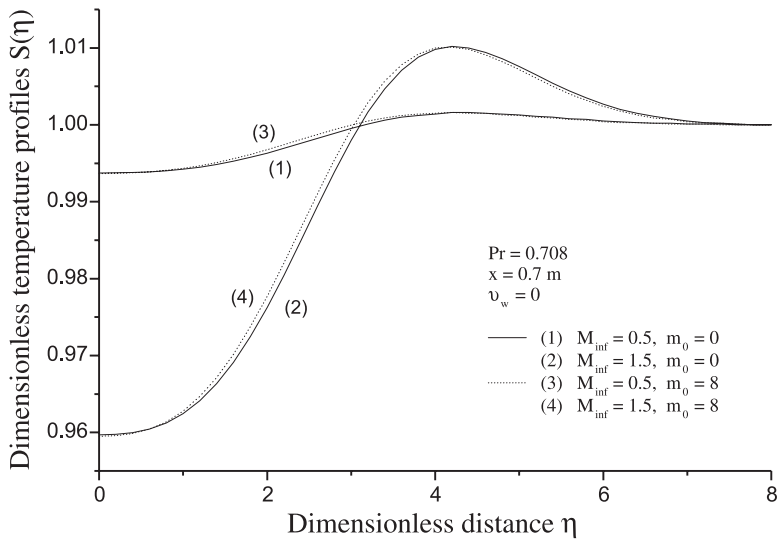

Fig. 8. Variations of the dimensionless temperature profiles $S(\eta)$ for $M_\infty = 0.5$; $m_0 = 4.0$; and $\upsilon_w = 0$, <0, >0.

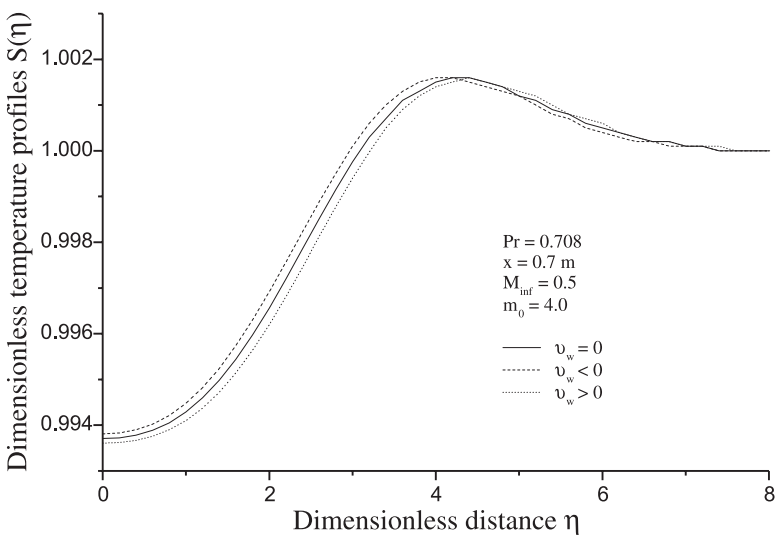

free-stream, the presence of a magnetic field decreases the temperature of the fluid but the opposite is true in the interior of the boundary layer. The influence of suction and (or) injection on the thermal boundary layer is shown in Figs. 8 and 9. In the neighbourhood of the wall, the temperature of the fluid is greater in the case of suction ($\upsilon_w < 0$) than the corresponding one in the case of an impermeable wall ($\upsilon_w = 0$) or in the case of injection ($\upsilon_w > 0$). However, the converse holds true approaching the free stream. The combined influence of suction and (or) injection and the applied magnetic field on the temperature field is exhibited in Fig. 9. It is observed that in the case of suction ($\upsilon_w < 0$) and when $\eta = 3$ and m_0 is increased from 0. to 8. there is a 0.033% increase in the value of S, whereas under similar circumstances the corresponding increase in the case of injection ($\upsilon_w > 0$) is 0.053%. Therefore, the percentage change in the value of $S\,(0.7,\ 3.0)$ between the cases $m_0 = 0.$, $\upsilon_w > 0$

Fig. 9. Variations of the dimensionless temperature profiles $S(\eta)$ for $M_\infty = 0.5$; $m_0 = 0\ 8$; and $\upsilon_w = 0, <0, >0$.

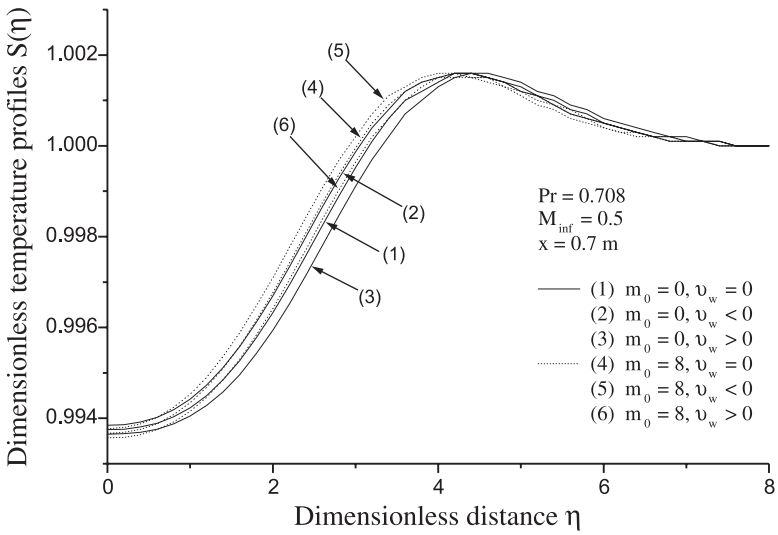

and $m_0 = 8.$, $\upsilon_w < 0$ is 0.109% . We should be reminded here that the total energy H is defined as $H = H_e S\left(H_e(x) = c_p T_e(x) + \frac{1}{2}u_e^2(x)\right)$. So, although the percentage changes in S are very small this does not mean that the corresponding changes in H are small.

The most important quantities in aerodynamics are the skin friction coefficient and the rate of heat-transfer coefficient. In our case the flow is adiabatic. So, the skin friction coefficient can be defined as

$$C_{f_x} = \frac{\tau_w}{\frac{1}{2}\rho_e u_e^2} \qquad \text{where} \qquad \tau_w = \left[\mu \frac{\partial u}{\partial y}\right]_{y=0} \tag{38}$$

Using (22), (23), and (27), these quantities can be written as

$$C_{f_x} = \frac{2C_w}{\sqrt{R_x}} f_w'' \tag{39}$$

where $f_w'' = f''(x, 0)$ is the wall-shear parameter.

Hence, the drag D on the plate, can be defined by the relation

$$D = \int_0^b \int_0^{x^*} \left[\mu \frac{\partial u}{\partial y}\right]_{y=0} \mathrm{d}x\, \mathrm{d}z \tag{40}$$

where b denotes the width of the plate and x^* the distance of the point of separation from the leading edge of the plate. Consequently, the drag D, per unit width of the plate, can be calculated by the expression

$$D = \int_0^{x^*} \frac{C_w f_w''(x, 0)}{\sqrt{R_x}} \rho_e(x) u_e(x)\, \mathrm{d}x \tag{41}$$

where $C_w = \rho_w \mu_w / \rho_e \mu_e$ and is a function of x.

So, Figs. 10 and 11 show the variations of the dimensionless wall-shear parameter f_w'' against the distance x for different values of the magnetic parameter m_0 and free-stream Mach number M_∞ for the case of an impermeable wall and for continuous suction and (or) injection imposed at the wall. The corresponding variations for the case of continuous or localized suction and (or) injection are shown in Figs. 12–14. The values of D for each case are also shown in these figures.

Fig. 10. Variations of the wall-shear parameter f''_w for $M_\infty = 0.5$; $m_0 = 0$ and 8; and $\upsilon_w = 0$, >0, <0.

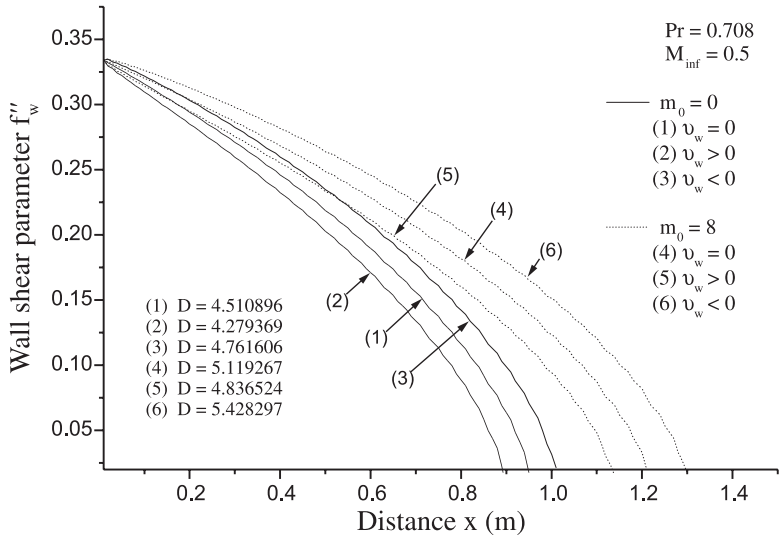

Fig. 11. Variations of the wall-shear parameter f''_w for $\upsilon_w = 0$; $m_0 = 0$ and 8; and for $M_\infty = 0.375$, 0.75, and 1.5.

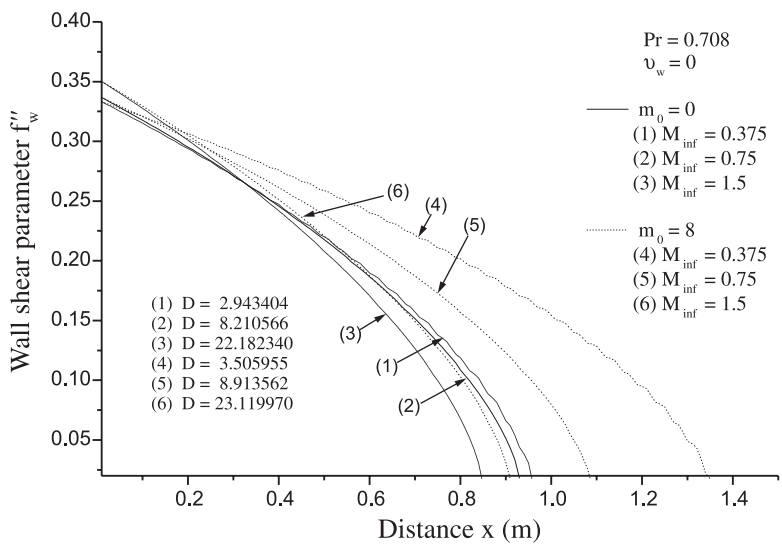

From Fig. 10, we can conclude that the presence of a magnetic field always helps in increasing frictional drag from the plate either in the case of suction and (or) injection or in the case of an impermeable plate. Also, application of suction moves the separation point towards the tail of the plate whereas the opposite is true in the case of injection. We can also conclude from Fig. 11 that in the hydrodynamic case ($m_0 = 0$), the separation point x^* always moves towards the tip of the plate as the free-stream Mach number increases and that this displacement is greater for higher values of M_∞. This is also true in MHD ($m_0 = 8$) but this displacement is higher for small values of M_∞. It is worth emphasizing here that for every value of the free-stream Mach number application of the magnetic field moves the separation point towards the tail of the plate.

Figure 12 presents the variations of the wall-shear parameter f''_w for an impermeable wall as well

Fig. 12. Variations of the wall-shear parameter f''_w for $M_\infty = 0.5$, $m_0 = 0$ and 8, and $\upsilon_w = 0$ and for $\upsilon_w < 0$ continuous or localized at $x_s = 0.7$.

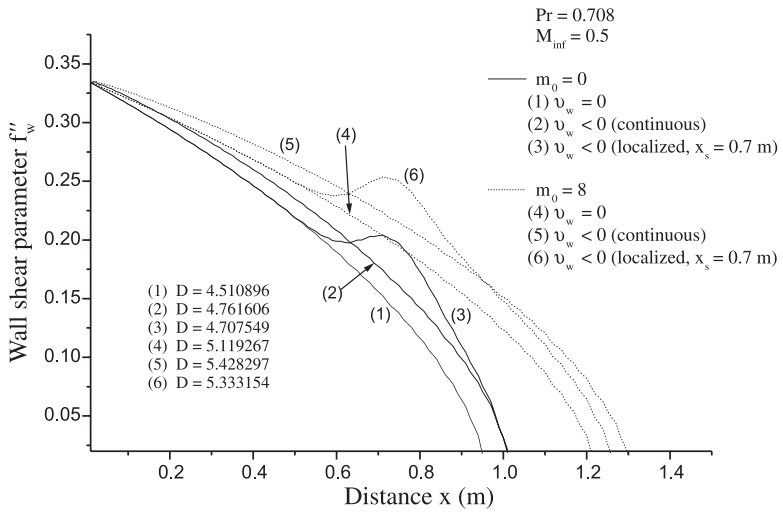

Fig. 13. Variations of the wall-shear parameter f''_w for $M_\infty = 0.5$; $m_0 = 0$; $\upsilon_w = 0$; and localized suction at $x_s = 0.4$, 0.6, 0.8, and 0.9.

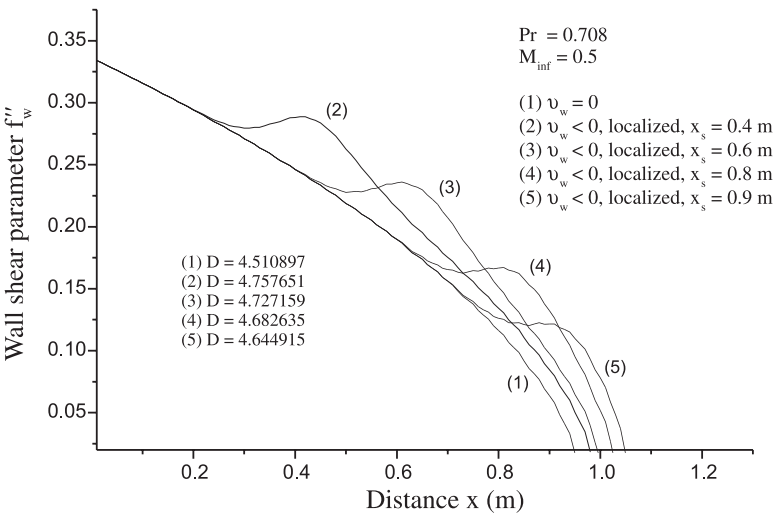

as for the case of continuous or localized suction for $m_0 = 0$ and $m_0 = 8.0$ at $x = 0.7$ m. It is observed that application of localized suction instead of continuous suction helps in decreasing the drag D and in moving the separation point x^* towards the tip of the plate; this fact is more evident in the magnetohydrodynamic case ($m_0 = 8$). It is worth emphasizing here the difference in the values of the fluid volume flux, through the plate, between the case of continuous and localized suction. According to (31), in the case of localized suction the fluid volume flux through a slot of width $2s$, is $Q_\ell = \sqrt{\pi}\, s^2 A_s$. In the case of continuous suction, the corresponding fluid volume flux is $Q_c = \upsilon_w x^*$. To be more specific, for $s = 0.1$ m and $A_s = 5 \times 10^{-5} u_\infty$, Q_ℓ is equal to $8.86 \times 10^{-7} u_\infty$, whereas in the case of continuous suction with $\upsilon_w = 10^{-5} u_\infty$ and for $x^* = 1$ m the corresponding fluid volume flux Q_c is equal to $10^{-5} u_\infty$. Figure 13 shows that application of localized suction at different locations x_s

Fig. 14. Variations of the wall-shear parameter f''_w for $M_\infty = 0.5$, $m_0 = 0$ and 8, $\upsilon_w = 0$, and localized suction and localized injection at $x_s = 0.9$ and 0.3, respectively.

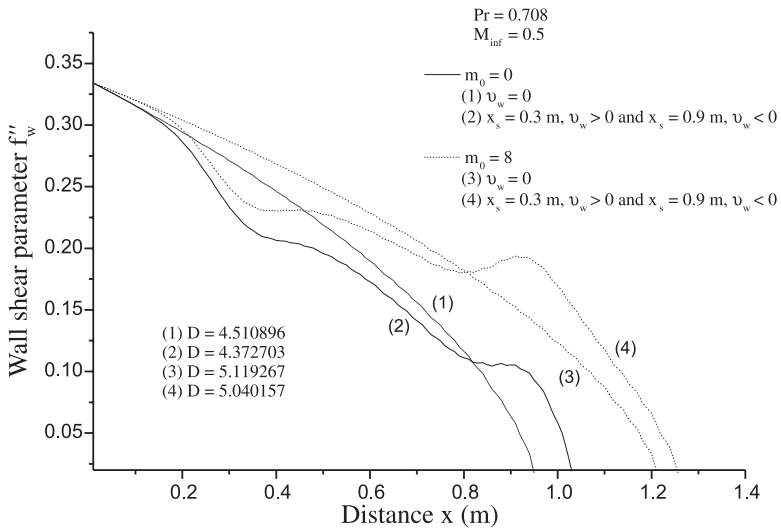

from the leading edge of the plate moves the separation point x^* downstream and reduces the frictional drag D. Finally, Fig. 14 shows the combined influence of the magnetic field and localized suction and (or) injection on the wall-shear parameter f''_w. It is concluded that application of localized suction and localized injection at the locations $x_s = 0.9$ m and $x_s = 0.3$ m, respectively, moves the separation point towards the tail of the plate and reduces frictional drag. The above analysis confirms the assertion that the technique of localized suction and (or) injection is still an effective method for boundary-layer control [5,33] and becomes more effective when the fluid is subjected to an applied magnetic field.

5. Concluding remarks

We summarize the important results concerning the wall-shear parameter and frictional drag as follows.

The presence of a magnetic field always increases frictional drag on the wall either in the case of suction and (or) injection or on an impermeable wall but moves the separation point towards the tail of the plate.

Application of magnetic field moves the separation point towards the tail of the plate for every value of the free-stream Mach number. This displacement is greater for small values of M_∞.

Localized suction at different locations from the leading edge of the plate helps in decreasing the drag and in moving the separation point towards the tail of the plate. This is more evident in the MHD case.

The combined influence of the magnetic field, localized injection, and localized suction moves the separation point towards the tail of the plate reducing frictional drag.

Acknowledgments

The authors are grateful to the referees for making useful comments for improving this article.

References

1. G.E.A. Meier. *In* Proceedings of the CISM Courses and Lectures on Control of Flow Instabilities and Unsteady Flows, Udine, Italy. No. 369. September 18–22, 1995. *Edited by* G.E.A. Meier and G.H. Schnerr. Springer-Verlag, New York. 1996. pp. 203–233.
2. F. Hirt and H. Thomann. J. Fluid Mech. **171**, 547 (1986).
3. P. Dengel and H.H. Fernholz. J. Fluid Mech. **212**, 615 (1990).
4. P.R. Spalart and J.H. Watmuff. J. Fluid Mech. **249**, 337 (1993).
5. D. Arnal. *In* Proceedings of the CISM Courses and Lectures on Control of Flow Instabilities and Unsteady Flows, Udine, Italy. No. 369. September 18–22, 1995. *Edited by* G.E.A. Meier and G.H. Schnerr. Springer-Verlag, New York. 1996. pp. 119–153.
6. N. Kafoussias, A. Karabis, and M. Xenos. Inter. J. Eng. Sci. **37**, 1795 (1999).
7. V.J. Rossow. NACA TN 3971, May 1957.
8. J.H. Davidson, F.A. Kulacki, and P.F. Dunn. Handbook of single-phase convective heat transfer. *Edited by* S. Kakac, R.K. Shah, and W. Aung. John Wiley & Sons, New York. 1987. pp. 9.1–9.49.
9. J.M.G. Chanty. J. Thermoph. Heat Transfer, **8**(4), 795 (1994).
10. D.D. Haldavnekar, S.S. Santpur, and V.M. Soundalgekar. Modeling, simulation & control B: Mechanical and Thermal Engineering, Materials & Resources, Chemistry, **54**, 1 (1994).
11. J.S. Chiou and H.N. Kao. Appl. Math. Modelling, **18**(2), 679 (1994).
12. S. Suwa and Y. Sasaki. Trans. Jpn. Soc. Aeron. Space Sci. **37**(115), 42 (1994).
13. A.K. Kalkan and G. Talmage. I. J. Heat Mass Transfer, **37**(3), 511 (1994).
14. K. Kinoshita, K. Tsunoda, and K. Yoshikawa. Heat Transfer Jpn. Res. **23**(3), 230 (1994).
15. C.R. Lin and C.K. Chen. Int. J. Eng. Sci. **31**(2), 2511993).
16. R.S.R. Gorla, J.K. Lee, S. Nakamura, and I. Pop. Int. J. Eng. Sci. **31**(7), 1035 (1993).
17. P.D. Ariel. Acta Mech. **103**, 31 (1994).
18. P.D. Ariel. Acta Mech. **105**, 49 (1994).
19. T. Watanabe and I. Pop. Acta Mech. **105**, 233 (1994).
20. I. Pop, M. Kumari, and G. Nath. Acta Mech. **106**, 215 (1994).
21. N.G. Kafoussias and N.D. Nanousis. Can. J. Phys. **75**, 733 (1997).
22. M. Kumari. Int. J. Eng. Sci. **36**(3), 299 (1998).
23. M.E.S. Ahmed and H.A. Attia. Can. J. Phys. **76**, 391 (1998).
24. R.S.R. Gorla, H.S. Takhar, and A. Slaouti. Int. J. Eng. Sci. **36**(3), 315 (1998).
25. I. Pop and T.Y. Na. Mech. Res. Commun. **25**(3), 263 (1998).
26. K.A. Yih. Acta Mech. **130**, 147 (1998).
27. H. Schlichting. Boundary-layer theory. *Translated by* J. Kestin. 7th ed. McGraw-Hill, Inc. New York. 1979. pp. 130–132, 173, 267, 268, 383, 396.
28. G.W. Sutton and A. Sherman. Engineering magnetohydrodynamics. McGraw-Hill, Inc. New York. 1965. p. 423.
29. W.F. Huges and F.J. Young. The electrodynamics of fluids. John Wiley & Sons. Inc. New York. 1966. p. 573.
30. K.R. Cramer and S.I. Pai. Magnetofluid dynamics for engineers and applied physicists. McGraw-Hill, Inc. New York. 1973. p. 127.
31. T. Cebeci and P. Bradshaw. Physical and computational aspects of convective heat transfer. Springer-Verlag, Inc. New York. 1984. p. 75, 109, 420.
32. J.J. Bertin and M.L. Smith. Aerodynamics for engineers, Prentice-Hall Inc., New Jersey. 1979. p. 376.
33. D. Arnal. Int. J. Num. Methods Fluids, **30**, 193 (1999).
34. Y.M. Chung, H.J. Sung, and A.V. Boiko. Phys. Fluids, **9**(11), 3258 (1997).
35. F.M. White. Viscous fluid flow. 2nd ed. McGraw-Hill, Inc. Singapore. 1991. p. 28.